低合金钢焊缝金属的腐蚀行为

黄安国[1], 李志远[1], 余圣甫[1], 周龙早[1], 张国栋[2]
(1.华中科技大学 材料学院, 武汉 430074
2 武汉大学 动力与机械学院, 武汉 430072)

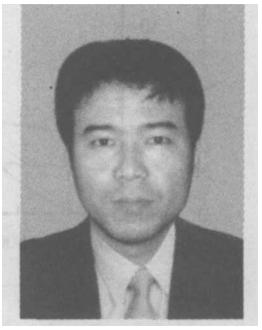

黄安国

摘 要: 研究了多种焊接工艺参数下, 母材分别为 16Mn和 X70钢的焊接接头各部位在 25℃空气中、25℃通 N_2 除氧 NACE溶液和 3.5% NaCl溶液中的腐蚀行为。结果表明, 针状铁素体腐蚀倾向较大, 但其腐蚀速度很慢; 焊接接头中针状铁素体数量对其腐蚀性能有着明显的作用, 较多数量的针状铁素体对应着较强的焊缝金属抗腐蚀能力, 但过量针状铁素体的出现可能会加快低合金钢焊接接头的腐蚀。

关键词: 低合金高强钢; 埋弧焊; 针状铁素体; 腐蚀; 极化电阻
中图分类号: TG405 文献标识码: A 文章编号: 0253-360X(2005)11-30-05

0 序 言

研究表明, 低合金钢焊缝金属中存在 60% ~ 80%的针状铁素体组织时, 焊接接头同时具有高的强度和良好的低温冲击韧度[1,2]。这解决了低合金钢与其焊接接头韧性匹配的问题, 使得低合金钢应用范围更加广泛。然而, 当低合金钢应用于工况恶劣的领域中, 如油气输送管线、海上钻井平台、跨海桥梁等工程, 其焊接接头与油、汽、海水等腐蚀介质直接接触, 此时, 焊接结构的耐腐蚀性往往决定着整个结构的服役寿命。目前, 对这一问题的研究尚未广泛开展[3~5]。因此, 针对低合金钢焊缝金属, 尤其是含大量针状铁素体组织的焊缝金属进行腐蚀规律的研究, 探讨防止腐蚀的措施, 具有相当重大的理论和实际意义。

1 试验方法和内容

1.1 试样的制取

试验选取了两种母材 16Mn和 X70钢, 为考察不同组织数量的低合金钢焊接接头的耐腐蚀性能, 试验采用两种焊接工艺进行施焊, 然后在两种腐蚀介质中进行腐蚀试验。

1.1.1 母材为 16Mn钢试样的制取

母材选用 16Mn钢, 板厚 16 mm。焊接材料选用直径为 φ4mm的 WDS2型埋弧焊丝, 该焊丝可促使焊缝中产生大量的针状铁素体。焊接前用手工电弧焊打底, 自动焊时焊接热输入分别为 2.79 kJ/mm和 4.96 kJ/mm。用线切割机分别截取纯母材、纯焊缝以及同时含有母材和焊缝的焊接接头三种试样, 见图 1, 试样尺寸为 50mm×10mm×4mm大小的长方形。用金相砂纸打磨, 抛光, 用丙酮清洗。母材和熔敷金属的成分见表 1。

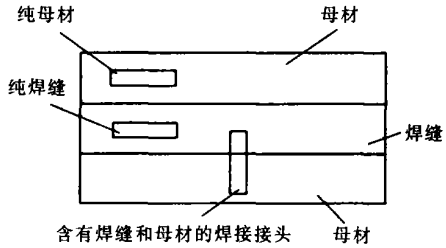

图 1 试样的示意图
Fig.1 Sketch map of samples

表 1 母材和焊缝金属化学成分(质量分数, %)
Table 1 Chemical compositions of base metal and weld metal of 16Mn steel

材料	C	Si	Mn	S	P	Ni	Mo	Ti
母材	0.20	0.30	1.60	0.016	0.016	-	-	-
熔敷金属	0.082	0.056	1.96	0.010	0.016	0.34	0.287	0.08

1.1.2 母材为 X70钢试样的制取

X70管线钢有两种试样, 第一种为直接从某钢管厂的 X70管线钢螺旋焊缝埋弧焊焊接生产现场

收稿日期: 2005-10-08
基金项目: 国家自然科学基金和上海宝钢集团公司联合资助基金项目(50334050)

截取的试样，焊缝中含有 70% －80%的针状铁素体组织，母材与焊缝金属成分见表 2。第二种试样焊接热输入为 4 18 kJ/mm，由于采用 H08A焊丝，所以焊缝中很少甚至不含针状铁素体。试样的切取与磨制同 16Mn钢试样。

表 2　母材和焊缝化学成分（质量分数，%）

Table 2　Chemical compositions of base metal and weld metal of X70 steel

	C	Si	Mn	P	S	Cr	Mo	Ni	Nb	V	Ti	Cu
母材	0 054	0 21	1 55	0 010	0 002 2	0 021	0 27	0 23	0 047	0 038	0 018	0 21
焊缝	0 052	0 22	1 39	0 014	0 003 6	0 026	0 30	0 15	0 031	0 028	0 19	0 16

1.1.3　腐蚀溶液的配制

根据实际需要配制了两种腐蚀介质，一种是 NACE溶液，其成分为 5% NaCl＋0 5% CH_3COOH，另一种溶液为人工海水，其成分为 3 5% NaCl溶液。

1.2　试样的腐蚀

两种材料分别在不同的条件下进行挂片腐蚀试验的。

（1）16Mn钢试样的腐蚀试验。该组试样采用了两组焊接工艺，根据腐蚀介质的不同，每种焊接热输入又分为两组。将已经制备好的试样分类编号分别放入 NACE和 3 5% NaCl溶液中，试样须完全浸泡在溶液中，不能相互接触，也不能碰到瓶壁与瓶底。放置好试样后，立即将广口瓶瓶塞盖上，以防止腐蚀溶液成分发生变化，然后将广口瓶放入温度为 50 ℃的恒温槽，腐蚀 150 h。

（2）X70管线钢试样的腐蚀。腐蚀的基本步骤与 16Mn钢试样腐蚀过程一致，不同的是，X70 管线钢试样的腐蚀温度为 20 ℃，腐蚀时间为 475 h。

1.3　极化曲线测量

应用华中科技大学化学系产 CT －2B 恒电位仪，采用三电极体系，参比电级为甘汞电极，辅助电极为铂电极，工电电极分别为 X70管线钢母材、X70管线钢含针状铁素体焊缝、X70管线钢不含针状铁素体焊缝，用 2号砂纸打磨，抛光；用酒精、丙酮擦拭，吹风吹干。试验温度为室温（25 ℃），浸泡 1 h后开始测试。电位扫描范围为 ±0 1 V，扫描速率为 0 5mV /s。试验所得数据用 Corrtest电化学测试系统软件进行弱极化拟合。

2　试验结果及讨论

2.1　母材为 16Mn钢的焊接接头腐蚀性

图 2a ~图 2f所示为两种焊接热输入焊缝试样和母材试样分别在 NACE和海水两种腐蚀介质中腐蚀形貌扫描照片。比较图 2a ~图 2d焊缝试样的微观腐蚀形貌可以看出，大热输入量的焊缝试样腐蚀面明显的凸凹不平，其中凸出部分为晶界或者是组织较细小针状铁素体组织，凹下部分组织是较为粗大的块状铁素体组织；小热输入焊缝试样的腐蚀面相对较为均匀，晶界处仍然是难以腐蚀的地方，但也可以看到极少量的点蚀孔。从图 2c还可看出在腐蚀完全的大晶粒的底面有较多微小点蚀孔，形状各异，或呈狭长状，或呈圆形。另外，还可看出，虽然各种组织都有不同程度的腐蚀，但较大的晶粒腐蚀较深，而晶界明显高出于腐蚀面。

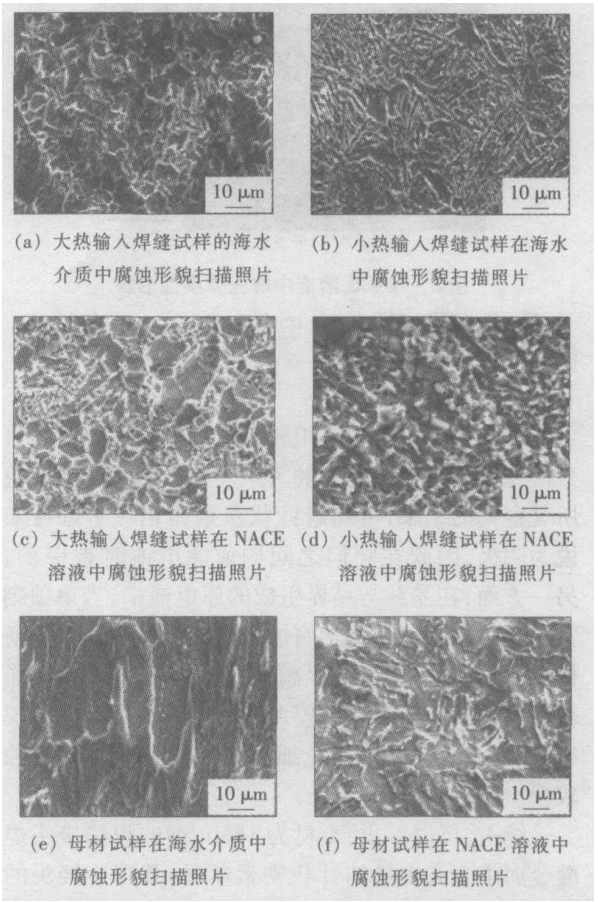

图 2　两种焊接热输入试样和母材分别在 NACE和海水两种腐蚀介质中腐蚀形貌扫描照片

Fig 2　SEM of corroded samples in 3 5% NaCl and NACE solutions

造成这种现象的原因在于钢材或焊缝中存在不可避免的杂质。母材的组织和碳原子分布较均匀，晶界由于原子排列较为疏松而紊乱更容易富集杂质原子，产生所谓晶界吸附和晶界沉淀，导致晶界比晶粒内更活泼，具有更负的电极电位值，成为了原电池的阳极而被腐蚀。但在焊缝金属中，对于针状铁素体来说，其晶界正是一层富碳的薄膜。碳在金属中是以 Fe_3C 的形式存在，它的电位一般来说要比晶内铁素体基体电位高，因此在电解质溶液中会形成原电池，Fe_3C 是阴极，铁素体是阳极，于是晶界得到了保护，而晶内组织腐蚀较快。图 3给出了 NACE腐蚀介质中珠光体的腐蚀形貌，珠光体是由渗碳体（Fe_3C）与铁素体组成，由图可以清晰地看出铁素体已被腐蚀完全，而留下了一层一层片状的渗碳体，这也正说明了在 Fe_3C 与铁素体的对偶腐蚀体系中，渗碳体具有更高的电极电位成为阴极而被保护。

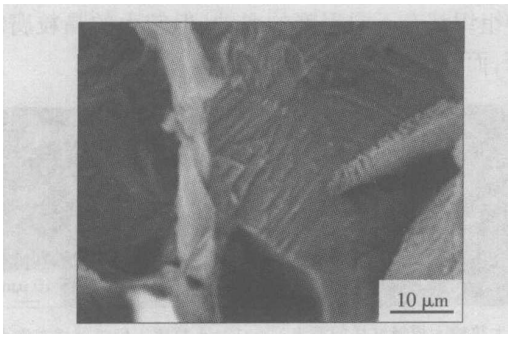

图 3 NACE溶液中珠光体腐蚀形貌

Fig. 3 SEM of pearlite microstructure corroded in NACE solution

焊缝金属中粗大组织较晶粒细小的组织腐蚀更为严重是因为腐蚀速率的关系。根据图 2腐蚀形貌所观察到的结果，可判定针状铁素体相对于母材来说为阴极，因此在它们之间构成原电池时被保护。另一方面，在晶粒与晶界组成的原电池中，当单独剩下晶界时发生的是化学腐蚀，腐蚀速度较慢，要重新构成原电池，必须使晶界腐蚀穿孔露出晶粒后才能获得，而图 2c表明组织较大的晶粒更易出现点蚀现象，因此，在实际中，晶粒细小区域或者晶界处腐蚀较慢。

综上，可以看出，母材为 16Mn钢的焊接接头焊缝金属中含有大量的针状铁素体时，其焊接接头的耐蚀性明显优于母材及焊接热影响区，这对于局部耐蚀性的提高是有好处的，但对于整体工程结构来讲，焊缝金属中针状铁素体数量过多反而会加速母材的腐蚀。

2.2 母材为 X70钢各试样腐蚀形貌的描述

图 4a~图 4f所示为母材为 X70钢的工艺参数不同的焊缝、焊缝＋热影响区和母材试样在 NACE介质中腐蚀形貌扫描照片，其中图 4e为图 4a放大 2 000倍后的扫描照片。

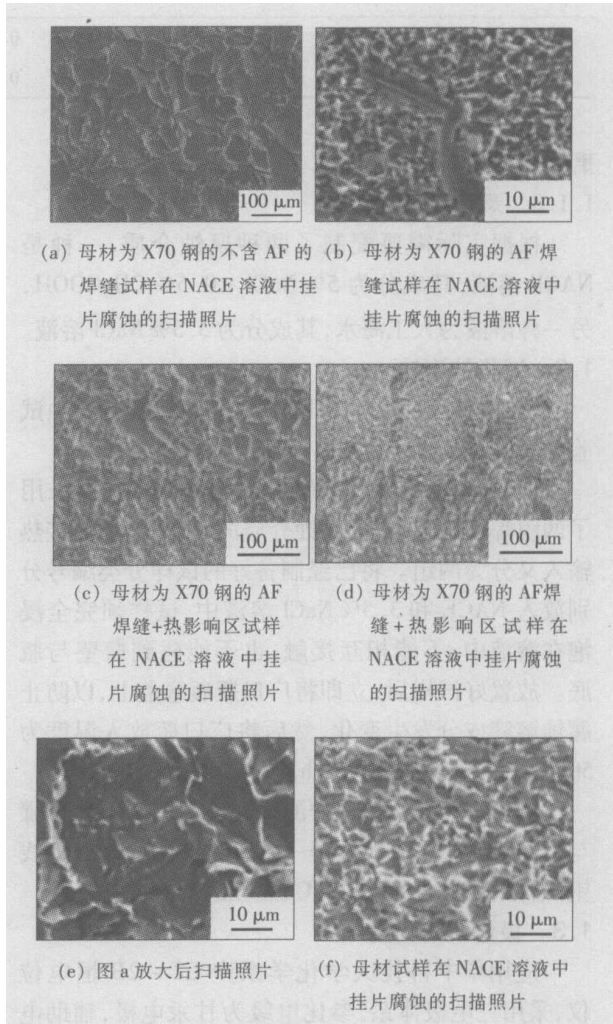

图 4 各试样在 NACE溶液中挂片腐蚀的扫描照片

Fig. 4 SEM of corroded samples for X70 steel in NACE solution

纵向比较图 4可发现，当焊缝金属中不含有针状铁素体时，其焊缝金属的腐蚀情况甚至劣于母材，在其粗大的焊缝金属组织中仍然可看到大量的点蚀坑，在图 4e中可清晰地看出，点蚀坑不仅分布在组织的底面上，晶界上同样分布较多；而针状铁素体组织焊缝试样中，焊缝金属与母材的腐蚀性能均优于热影响区，这既说明了 X70钢的耐腐蚀性能较强而被广泛用于各种恶劣环境工况下，但同时必须注意到 X70钢焊接接头热影响区仍然存在着很大隐患，这也正是要大力发展针状铁素体钢的必要性。此外，在图 4b、图 4d中还可看出，针状铁素体组织的

晶界依然保留，而焊缝金属内的先共析铁素体组织总是先于针状铁素体组织被腐蚀，这是因为先共析铁素体本身就是在原奥氏体晶界上形核并长大的，奥氏体晶界不像针状铁素体组织的晶界那样是一层富碳的薄膜，而是原子排列较为疏松晶粒内部更为活泼的界面，因而与其内的针状铁素体组织组成微小的原电池，当奥氏体内针状铁素体数量较多形成较多的界面时，会形成大阴极小阳极的腐蚀状态，大大增加了腐蚀速率，导致先共析铁素体被腐蚀。

横向比较图 4c和图 4d 还可发现，含针状铁素体组织较多的试样，其热影响区的腐蚀形貌较不含针状铁素体组织试样的焊接热影响区的腐蚀形貌更为恶劣，这主要是因为图 4d中焊缝金属与焊接热影响区的成分、形态上的差异相对于图 4c中的更为大，腐蚀速度更快。这表明针状铁素体焊接接头腐蚀性能最差区域应是焊接热影响区而非焊缝本身，另外，再一次间接的证明了并非针状铁素体数量越多就越有利于焊接接头的抗腐蚀性能。

2.3　各试样腐蚀倾向与腐蚀速率的探讨

表 3给出了相应的弱极化区（3参数）Tafel曲线拟合的结果，图 5为母材为 X70钢的不同试样在 NACE溶液中的极化曲线。

由图 4和表 3可知，三种试样在 NACE溶液中两两组成的腐蚀电偶对中，针状铁素体焊缝金属与母材的差值最大，因而它们之间最易发生腐蚀，针状铁素体焊缝作为阴极被保护，并且在腐蚀开始的时候，母材腐蚀速率也很快，因此同样条件下，必然它们组成的电偶对腐蚀的更加严重。表 3指出，针状铁素体焊缝金属的腐蚀电位最负，腐蚀电位差是热力学参数，是腐蚀过程的驱动力，差值越大表明发生

表 3　弱极化区 Tafel曲线拟合的结果

Table 3　Fitted results of Tafel curve in weak polarization zone

腐蚀介质	试样	腐蚀电位 U/V	腐蚀速率 v/(mm·年$^{-1}$)	腐蚀电流密度 S/(mA·cm^{-2})
25℃空气 NACE溶液中	AF焊缝	-0.596	0.488 7	0.041 7
	无 AF焊缝	-0.589	0.224 5	0.019 1
	母材	-0.600	0.708 0	0.060 4
25℃通氮除氧 NACE溶液中	AF焊缝	-0.639	0.038 6	0.003 3
	无 AF焊缝	-0.632	0.026 5	0.002 3
	母材	-0.643	0.044 5	0.003 8

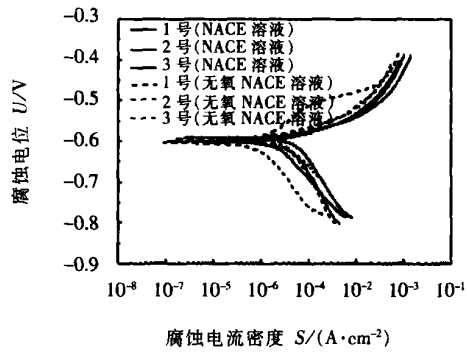

图 5　母材为 X70钢各试样在 NACE溶液中极化曲线（1，母材，2，AF焊缝，3，无 AF焊缝）

Fig. 5　Polarization curve of various samples of X70 Steel in NACE solution(1, Base metal; 2, Weld metal including AF microstructure; 3, Weld metal excluding AF microstructure)

腐蚀的倾向越大，但并不能认为腐蚀速率就大。腐蚀速度还取决于阴、阳极的极化率，这是发生腐蚀的阻力。试验结果与极化曲线表明，AF焊缝金属的腐蚀倾向很大，但腐蚀阻力也很大。另外，从表 3中还可看出，置露于空气中的试样，其腐蚀速度比通氮除氧溶液中的腐蚀速度快很多，这说明 X70钢及其焊接接头对吸氧腐蚀的敏感程度较高。

3　含大量针状铁素体组织的低合金钢焊缝金属腐蚀机理的探讨

含大量针状铁素体组织的焊缝金属的腐蚀倾向很大、腐蚀速率很小的原因与针状铁素体组织本身的特点有很大的关系。针状铁素体（AF）晶粒是由非金属夹杂物核心、包围在夹杂物四周的铁素体和外围的富碳层所组成的组织，其中的富碳层可以看作是 AF晶粒的晶界。一般认为，由于晶界化学成分的不均匀性，会导致晶界比晶粒内更为活泼，具有更负的电极电位值。所以，晶界成为微电池的阳极，腐蚀首先从晶界开始[6]。但是，针状铁素体的晶界里面富含 Fe_3C等杂质，它的电位要比晶内铁素体基体电位高，因此在电解质溶液中形成原电池时，Fe_3C是阴极，铁素体是阳极，于是晶界得到了保护，而晶内组织腐蚀较快[7]。在试验中可以发现，在两种介质的腐蚀过程中，AF的富碳层难以腐蚀，晶界绝大部分保留，也就是说 AF组织的晶界相对于其它组织的晶界具有更高的电极电位而成为阴极，加之数量众多，因此在局部的地方（如单个的奥氏体晶粒内部）构成大的阴极面积，从而降低了自身的

腐蚀速率而被保护,因而针状铁素体焊缝金属总是表现得更耐腐蚀。

另一方面,针状铁素体是通过切变机制生成的,转变过程中有剧烈的塑性变形发生,伴随产生大量的位错。文献[5]指出,在位错处形成腐蚀孔并不断长大的几率远较无位错处的金属表面为大,腐蚀孔的形成更易于发生于位错部位。因此,针状铁素体组织的腐蚀倾向比较大。

4 结 论

(1)针状铁素体腐蚀倾向较大,但其腐蚀速度不快,甚至很慢,这与针状铁素体组织本身的特征有关。针状铁素体内含有大量的位错成为腐蚀孔形核处,导致针状铁素体具有很大的腐蚀倾向。但另一方面,针状铁素体晶界为一富碳层的薄膜,在腐蚀过程中,富碳层晶界减缓了针状铁素体的化学腐蚀。在与其它组织组成微观腐蚀原电池时,富碳层的存在又使得针状铁素体组织成为阴极而得到保护,针状铁素体的耐腐蚀性能较其它组织好。

(2)焊接接头中针状铁素体数量对其腐蚀性能有着明显的作用。一般说来,较多数量的针状铁素体对应着较强的焊缝金属抗腐蚀能力,但过量针状铁素体的出现可能会加快金属焊接接头的腐蚀。这一方面是因为针状铁素体焊缝金属与母材或焊接热影响区形成宏观原电池,加快了母材或焊接热影响区的腐蚀;另一方面则是数量众多、组织细小的针状铁素体与其它组织形成原电池时,提供了大的晶界面,造成了大阴极小阳极的腐蚀状态从而加速了焊缝金属的腐蚀速率。因此,在针状铁素体焊缝金属中不能把焊缝腐蚀速率快慢与针状铁素体的耐腐蚀能力等价起来。也因此,在 X70钢的焊接接头中,应在保证强度与韧性的前提下,控制针状铁素体的含量,以减小局部腐蚀电池中的阴极面积。这对实际的工程建设有着相当重要的意义。

参考文献:

[1] 王祖滨,宋 青. 世纪之交看低合金高强度钢的发展[J]. 钢铁, 2001, 36(9): 66-70.

[2] 余圣甫,雷 毅,黄安国,等. 氧化物技术及其冶金应用[J]. 材料导报, 2004, 18(8): 50-52.

[3] Huang Herhsing, Tsai Wenta, Li Jutung. The influences of microstructure and composition on the electrochemical behavior of A516 steel weldment[J]. Corrosion Science, 1994, 36(7): 1027-1031.

[4] Huang Herhsing, Lee Jutung, Tsai Wenta. Effect of H_2S on the electrochemical behavior of steel weld in aacidic cchloride solutions[J]. Materials Chemistry and Physics, 1999, 58(7): 177-181.

[5] 黄安国,王永生,李志远,等. 针状铁素体焊缝金属腐蚀行为的研究[J]. 材料保护, 2004, 37(3): 6-8.

[6] 方坦纳 M G 著. 腐蚀工程[M]. 左景伊译. 北京:化学工业出版社, 1982. 70-173.

[7] 魏宝明. 金属腐蚀理论及应用[M]. 北京:化学工业出版社, 1984. 176-207.

作者简介:黄安国,男,1975年 9月出生,工学博士,讲师。主要从事新型焊接材料的开发和焊缝组织行为特征的研究和模拟工作,发表论文 10余篇。

Email: huang-anguo@163.com

Key words: high temperature polymer matrix composite material; ceramic coating; erosion; thermal-resistance coating

Dynamic behavior of plasma in CO_2 laser welding of stainless steel

DUAN Ai-qin[1,2], CHEN Li[1,2], WANG Ya-jun[2], HU Lun-ji[1] (1. Huazhong University of Technology and Science, Wuhan 430074, China; 2. BAMTRI, Key laboratory for high energy density beam processing technology, Beijing 100024, China). p17 - 20

Abstract: Laser induced plasma is an important physical phenomenon in laser deep penetration welding. It has stronger relationsip to stability of process, quality of weld, and efficiency of laser energy. In this paper, two methods were used to study the dynamic behavior of plasma and the influences on stability of welding process. These methods were high-speed camera and optical signal monitoring. The results showed that the dynamic process of plasma can be divided into four steps, (1) material vaporing; (2) plasma increasing; (3) plasma bombing and separating; (4) plasma scattering. The main reason affected welding process stability is the fluctuation of plasma between non-penetration and penetration process.

Key words: Laser welding; laser induced-plasma; high-speed camera; optical signal

Weld residual stress distribution of GH536 superalloy with EBW measuned by Mathar method FU Peng-fei, LIU Fang-jun, FU Gang, MAO Zhi-yong (Key Laboratory of high energy density beam processing technology, Beijing Aeronautical Manufacturing Technology Research Institute, Beijing 100024, China). p21 - 23

Abstract: Electron beam welding is applied to manufacturing many superalloy components of aeroengine, but the researches of weld residual stress were very few for those components. In this paper, weld residual stress of GH536 superalloy components with EBW were measured by Mathar method. Test results showed that residual stress is low in the weld and its distribution accords with the traditional rules. This research can accumulate experiences and properties data for manufacturing aeroengine components with EBW.

Key words: GH536 superalloy; electron beam welding; hole drilling method; residual stress

Real-time monitor system based on virtual instrument technology for laser welding ZHANG Pu, PENG Qi-zhi, KONG Li (Huazhong University of Technology and Science, Wuhan 430074, China). p24 - 26

Abstract: The laser deep penetration welding monitoring system based on the virtual instrument technology was introduced. The component of hardware and the development of software were illuminated. Three signals of ultraviolet light, infrared light and acoustic signal acquired by three special sensors. The raw data were processed dy DSP, multi-sensors data fusion was done by neural network algorithm, and the reliable result of welding quality was oslained. The experimental data proved the system's validity and stability.

Key words: virtual instrument; laser welding; data fusion

Optimization selection of power source frequency in high frequency induction brazing HE Peng, LIU Duo, FENG Ji-cai (National Key Laboratory of Advanced Welding Production Technology, Harbin Institute of Technology, Harbin 150001, China). p27 - 29

Abstract: Appropriate frequency of high frequency power source shoulded be selected to obtain perfect soldered joint during high frequency induction brazing according to the physical performance of joint materials. Numerical selection model for the frequency and its arrange of high frequency induction heating power source was set up by means of numerical analysis. It showed that numerical analysis can be used as an important artifice for design of high frequency power equipment. Compared the analytical results from the numerical model with that of the traditional formula, it showed that the former is more accurate. Because the latter was derived from the plane electromagnetic wave spreading characteristic in electro-conductive inter-media, it was more suitable for the frequency selection of board structure high frequency induction heating. But for frequency selection of pipe-structure or more complex structure high frequency induction heating, the numerical analytical method will be better.

Key words: high frequency induction brazing; power frequency; numerical analysis

Corrosion behavior of weld metal of low-alloy steel HUANG An-guo[1], LI Zhi-yuan[1], YU Sheng-fu[1], ZHOU Long-zao[1], ZHANG Guo-dong[2] (1. School of Materials Science and Engineering, Huazhong University of Science and Technology, Wuhan 430074, China; 2. School of Power and Mechanic, Wuhan Uniersity, Wuhan 430072, China). p30 - 34

Abstract: Two welding heat input were applied to 16Mn and X70 steel by SAW. The corrosion behavior of weld metal was investigated in two kinds of solution, NACE and 3.5% NaCl, respectively. The results show that corrosion tendency of acicular ferrite (AF) in weld is greater than other microstructures, but its corrosion velocity is slowly. The corrosion resistance of weld metal with AF increases with the increasing of ac-

icular ferrite fraction, but too much acicular ferrite microstructures leads to accelerate corrosion of weld in HSLA.

Key words: high strength low alloy steel; SAW; acicular ferrite; corrosion; polarization resistance

Mathematical model of the stable full penetration laser welding for titanium alloy sheet CHEN Li[1,2], HU Lun-ji[1], GONG Shui-li[2] (1. Huazhong University of Science and technology, Wuhan 430074, China; 2. Key Lab for High density beam manufacture technology, Beijing aeronautic manufacturing technology research institute, Beijing 100024, China). p35 - 38

Abstract: The macrostructure of laser welding for titanium alloy was investigated in this paper. The results show that unstable full penetration will occur because of influence of laser induced plasma, even though laser welding parameters were stable. This phenomenon was characterized by perfect weld surface, and unstable weld back that part penetration and full penetration formed by turns. It is assumed that unstable full penetration was intrinsic for laser penetration welding and depended on significantly the drilling speed during the keyhole forming. According to the energy balance on keyhole wall, the mathematical model for the smallest laser power density that made the stable full penetration weld was suggested in this paper, which allowed laser power density to be related to material properties, sheet thickness the, drill speed and laser welding speed. The computed results were corresponded with the experimental results.

Key words: titanium alloy; laser welding; full penetration; welding stability calculation

Influnce of process parameters on appearance of plasma-melt-sprayed WC-17%Co coatings ZHAO Min-hai, LIU Ai-guo, GUO Mian-huan, LIU De-Jian, (National Key Laboratory of Advanced Welding Production Technology, Harbin Institute of Technology, Harbin 150001, China). p39 - 42

Abstract: Ceramic coatings can be metallurically bonded to metal sabstrate with plasma-melt-spraging, which has virtue of both plasma spray and harfacing. Coralt-based WC is hard, wear-reristant, corrosion-resistant and thermal-resistant. WC-17% Co coating was plasma-melt-sprayed on Q235 substrate. Influnce of proceis parameters (angle between plasma melting torch and spraying torch, distance between the plasma torch and the substrate, velocity of melting and spraying and feeding rate of powder) on appearamce of the coating was investigated, and the pavameters were optimized. Metallurgically bonded coating without defects was obtained.

Key words: plasma melt spraying; WC-17% Co coating, parameter, appearame

Microstructures and properties of TC4 alloy joints welded by the electron beam welding XU Hong-ji[1], YIN Li-xiang[1], LI Jin-wei[2], XIE Ming[1] (1. School of Materials Science and Engineering, Dalian Jiaotong University, Dalian 116028, China; 2. Beijing Aeronautical Manufacturing Technology Research Institute, Beijing 100024, China). p43 - 46

Abstract: Microstructures and properties of TC4 alloy joints welded by electron beam welding were investigated with room-temperature tensile test, room-temperature notch tension test, microhardness test and metallographic analysis. The results showed that the joints with good performance of TC4 alloy may be obtained by means of electron beam welding (EBW). The tensile strength of welded joint is not less than that of the base metal, and the notch sensitive coefficient of the welded joint is less than 1. The hardness of the welded joint and the HAZ are higher than that of the base metal. The microstructure of the weld metal is α' phase (needle martensite) which was transformed from the primary coarse β matrix, and that of the HAZ was the mixture of fine needle martensite and the primary α phase.

Key words: TC4 alloy; electron beam welding; welded joint

Study on heat transfer of melt pool in laser keyhole welding WANG Hong[1,2], SHI Yao-wu[1], GONG Shui-li[2], (1. School of Materials Science and Engineering Beijing university of Technology, Beijing 100022, China; 2. Beijing aeronautical manufacture technology research institute, Beijing 100024, China). p47 - 50

Abstract: The shape of welding pool in laser deep penetration welding was calculated based on continuity equation, momentum conservation equation and energy conservation equation using FLUENT solver. Solidification/Melting model and $\kappa - \varepsilon$ model were used. Simulation results showed that the recoil pressure on the front wall of the keyhole is an important driving force of welding pool fluid flow because of large temperature gradient in the front part. The larger size of the solidification transition zone of welding pool in the liquid-solid interface was related to solidification heat.

Key words: laser welding; simulation; molten pool; titanium alloy